



ORIGINAL RESEARCH

Genes deregulated in giant cell arteritis by Nanostring nCounter gene expression profiling in temporal artery biopsies

Ilaria Ferrigno,^{1,2} Martina Bonacini ,² Alessandro Rossi,² Maria Nicastro,² Francesco Muratore ,^{3,4} Luigi Boiardi,³ Alberto Cavazza,⁵ Alessandra Bisagni,⁵ Luca Cimino,^{4,6} Angelo Ghidini,⁷ Giuseppe Malchiodi,⁸ Alessandro Zerbini,² Nicolò Pipitone,³ Carlo Salvarani,^{3,4} Stefania Croci ²

To cite: Ferrigno I, Bonacini M, Rossi A, *et al.* Genes deregulated in giant cell arteritis by Nanostring nCounter gene expression profiling in temporal artery biopsies. *RMD Open* 2024;**10**:e004600. doi:10.1136/rmdopen-2024-004600

► Additional supplemental material is published online only. To view, please visit the journal online (<https://doi.org/10.1136/rmdopen-2024-004600>).

IF and MB contributed equally.

CS and SC are joint senior authors.

Received 1 June 2024
Accepted 13 September 2024



© Author(s) (or their employer(s)) 2024. Re-use permitted under CC BY-NC. No commercial re-use. See rights and permissions. Published by BMJ.

For numbered affiliations see end of article.

Correspondence to

Dr Stefania Croci;
stefania.croci@ausl.re.it

ABSTRACT

Objective To identify differentially expressed genes in temporal artery biopsies (TABs) from patients with giant cell arteritis (GCA) with different histological patterns of inflammation: transmural inflammation (TMI) and inflammation limited to adventitia (ILA), compared with normal TABs from patients without GCA.

Methods Expression of 770 immune-related genes was profiled with the NanoString nCounter PanCancer Immune Profiling Panel on formalin-fixed paraffin-embedded TABs from 42 GCA patients with TMI, 7 GCA patients with ILA and 7 non-GCA controls.

Results Unsupervised clustering of the samples revealed two distinct groups: normal TABs and TABs with ILA in one group, 41/42 TABs with TMI in the other one. TABs with TMI showed 31 downregulated and 256 upregulated genes compared with normal TABs; they displayed 26 downregulated and 187 upregulated genes compared with TABs with ILA (>2.0 fold changes and adjusted p values <0.05). Gene expression in TABs with ILA resembled normal TABs although 38 genes exhibited >2.0 fold changes, but these changes lost statistical significance after Benjamini-Yekutieli correction. Genes encoding TNF superfamily members, immune checkpoints, chemokine and chemokine receptors, toll-like receptors, complement molecules, Fc receptors for IgG antibodies, signalling lymphocytic activation molecules, JAK3, STAT1 and STAT4 resulted upregulated in TMI.

Conclusions TABs with TMI had a distinct transcriptome compared with normal TABs and TABs with ILA. The few genes potentially deregulated in ILA were also deregulated in TMI. Gene profiling allowed to deepen the knowledge of GCA pathogenesis.

INTRODUCTION

Giant cell arteritis (GCA) is a systemic inflammatory disease affecting large-sized and medium-sized arteries. It is the most common vasculitis in people older than 50 years of age, and the ageing of immune and vascular cells

WHAT IS ALREADY KNOWN ON THIS TOPIC

- ⇒ Several molecules are known to be deregulated in temporal arteries from patients with giant cell arteritis (GCA) but high-throughput assays in temporal arteries are still scarce.
- ⇒ Temporal artery biopsies (TABs) can have different histological patterns of inflammation: transmural inflammation (TMI) is the most frequent pattern, while inflammation limited to adventitia (ILA) can be found in 7% of the positive TABs.

WHAT THIS STUDY ADDS

- ⇒ TABs with TMI had a distinct transcriptome compared with normal TABs and TABs with ILA.
- ⇒ TABs with ILA were heterogeneous: some samples had a transcriptome similar to normal TABs, while others clustered between normal TABs and TABs with TMI.
- ⇒ Novel molecules and pathways potentially involved in the pathogenesis of GCA were identified, and the deregulation of previously known ones was confirmed.

HOW THIS STUDY MIGHT AFFECT RESEARCH, PRACTICE OR POLICY

- ⇒ Nanostring nCounter gene profiling in TABs provided novel molecules likely involved in GCA pathogenesis, which could be further investigated to develop novel therapies.

are risk factors for the disease.¹ Diagnosis derives from the integration of clinical signs, laboratory data (increase in systemic markers of inflammation), histological features and imaging data. Temporal artery biopsies (TABs) are routinely performed to confirm the diagnosis, giving the invaluable opportunity to analyse the tissues affected by inflammation. TABs can exhibit different histological patterns of inflammation. Transmural

inflammation (TMI) is the most frequent pattern (78% of the positive TABs), characterised by leucocytes crossing the external elastic lamina, infiltrating the media towards the intima. Inflammation limited to adventitia (ILA) can be found in 7% of the positive TABs: leucocytes are confined to this layer, without medial involvement.² Whether ILA precedes TMI or represents distinct GCA subsets is unclear.

Glucocorticoids are the first-line treatment for GCA patients, irrespective of clinical presentations and inflammation patterns. However, many patients experience glucocorticoid-related adverse events. Moreover, more than half of patients develop flares during glucocorticoid tapering or after glucocorticoid discontinuation.³ Our understanding of GCA pathogenesis is growing, but it is still insufficient for precision medicine. Activation of vascular dendritic cells (DCs) coupled with the presence of disease favouring T lymphocytes seem both necessary for GCA development. Loss of arterial immune privilege allows the entry of monocytes and T cells into the arterial wall. T lymphocytes become activated and polarise in various subsets under the effects of several cytokines. Tissue-damaging macrophages expand, with the generation of multinucleated giant cells. Increased levels of cytokines, growth factors, proteases can ultimately lead to arterial remodelling, neoangiogenesis and intimal hyperplasia with lumen occlusion, wall dissection and aneurysm formation.^{4,5} Data on the pathogenic role of specific pathways in GCA derive from human artery-mouse chimaeras,⁶ TAB sections cultured *ex vivo*,⁷⁻⁹ primary cultures from TABs¹⁰ and clinical trials testing the efficacy of targeted therapies.¹¹

To advance precision medicine and discover additional targets for those patients who are refractory to the current therapies, it is necessary to increase the knowledge of the molecular features of GCA.¹² High-throughput assays are of help in this perspective, but they are scarce in TABs from GCA patients.¹³⁻¹⁶ This study aims to identify differentially expressed genes (DEGs) in inflamed TABs from patients with GCA compared with normal TABs from controls using the Nanostring nCounter gene profiling technology. Additionally, the study aims to increase the understanding of TMI and ILA histological patterns of inflammation in GCA.

PATIENTS AND METHODS

Patients and TABs

We retrospectively reviewed the clinical information of the patients who performed TABs at AUSL-IRCCS at Reggio Emilia (Italy) for a suspicion of GCA. We selected (1) patients with GCA and TMI naïve from therapy at the time of TABs; (2) patients without GCA and with normal TABs naïve from therapy at the time of TABs and (3) patients with ILA irrespective of therapy at the time of TABs. Patients with normal TABs did not have GCA based on medical evaluation at diagnosis and during the follow-up period performed by CS and FM. We retrieved

from the archives of the Unit of Pathology the corresponding formalin-fixed paraffin-embedded (FFPE) TABs. We reviewed each tissue specimen and we selected and processed those which were mainly composed of arterial tissue and had enough material: 64 TABs with TMI; 14 TABs with ILA; 18 normal TABs. After yield and quality control of the RNA samples, we were ultimately able to profile 46 TABs with TMI, 7 TABs with ILA and 7 normal TABs with Nanostring nCounter. We also included a validation cohort of patients with the above mentioned characteristics, whose snap frozen TABs were analysed by real-time PCR (n=7 patients with TMI, n=7 patients with ILA, n=7 patients with normal TABs). We recorded the following data: age at biopsy, sex, date of prednisone initiation, presence of cranial symptoms, visual symptoms, systemic signs/symptoms, polymyalgia rheumatica, erythrocyte sedimentation rate, C reactive protein, TAB histology.

RNA extraction from TABs

RNA was manually extracted using the AllPrep DNA/RNA FFPE kit (Qiagen, Hilden, Germany) from FFPE TABs (10 slices with 10 µm thickness for each sample). Tissue was deparaffinised using xylene. We optimised the protocol by adding a wash with 80% ethanol. Most of the RNA samples did not fulfil the requirements of purity and concentration for Nanostring nCounter assays: A260/280>1.8; A230/260>1.5 and concentration >33.3 ng/µL. Therefore, all the RNA samples were purified and concentrated with the RNA Clean & Concentrator kit in a final volume of 8 µL (Zymo Research, Irvine, California, USA). RNA was manually extracted using the RNA/DNA/Protein Purification Plus Kit (Norgen Biotek) from snap frozen TABs. RNA quantification was performed with NanoDrop instrument (ThermoFisher Scientific).

NanoString nCounter gene profiling

The expression of 770 genes was profiled in the samples through hybridisation with barcoded specific probes using the NanoString nCounter PanCancer Immune Profiling Panel (NanoString Technologies, Seattle, Washington, USA). 150 ng RNAs were analysed following the protocol suggested in the manual.

Data processing and statistical analysis

Raw data were processed with nSolver software V.4.0 (NanoString Technologies). Background thresholding using the negative control probes was applied, then data were normalised over the positive control probes and 18 housekeeper genes. Quality control analysis was performed using default parameters. Background thresholding was set up as the mean of the negative control probes plus two SD. Positive control probes A-F were included for calculating the normalisation factors as the ratios between the average of the geometric means and the geometric mean of each sample. The data were normalised for the RNA content selecting 18/40

housekeeping genes with the lowest coefficients of variation (<0.6): *AMMECR1L*, *CC2D1B*, *DHX16*, *DNAJC14*, *EDC3*, *ERCC3*, *FCF1*, *GPATCH3*, *GUSB*, *HDAC3*, *MTMR14*, *POLR2A*, *PPIA*, *SDHA*, *SF3A3*, *TLK2*, *TMUB2*, *ZKSCAN5*. The normalisation factors were calculated as the ratios between the average of the geometric means and the geometric mean of each sample.

Fold changes were calculated for each mRNA as the ratios between the geometric means of the normalised expression values in each group (ie, TAB histotypes). Differences in the normalised expression values between groups were analysed with the Mann-Whitney U test, and adjusted p values were obtained after correction for multiple testing using the Benjamini-Yekutieli procedure with IBM SPSS Statistics version V.29.0.1.0. Differentially expressed genes (DEGs) with fold changes >2.0 or <-2.0 and Benjamini-Yekutieli adjusted $p<0.05$ were considered significant. Non-detectable genes were identified as mRNAs expressed in a maximum of one sample.

GraphPad Prism software V.6 was used to analyse immune cell markers in TABs and real-time PCR data (Kruskal-Wallis test with Dunn's post-test and Fisher's exact test).

Bioinformatic analyses

Volcano plots were created using the web app VolcanoR.¹⁷ DEG lists were compared using Venn's diagrams (<https://bioinfo.gp.cnb.csic.es/tools/venny/index.html>). Unsupervised hierarchical clustering was carried out using the web tool ClustVis¹⁸ and applying the Euclidean average distances for both samples and genes. Preprocessing settings included logarithmic transformation ($\ln(x)$), row centering and no scaling. PCA was carried out using the web tool ClustVis¹⁸ based on the normalised expression of the 770 gene set. Values were logarithmic-transformed; no scaling was applied to rows; SVD with imputation was used to calculate principal components. DEGs were uploaded into the 'Database for Annotation, Visualisation and Integrated Discovery' (DAVID)¹⁹ to perform gene functional annotation clustering with high classification stringency based on REACTOME pathway database and Gene Ontology Biological Process knowledgebase. Specifically, the following parameters were selected: similarity term overlap=3; similarity threshold=0.85; initial and final group membership=3; multiple linkage threshold=0.5; enrichment threshold EASE=1.0. Homo sapiens was selected as background. Clusters with enrichment scores >8 and false discovery rates $<10^{-6}$ for the upregulated DEGs; enrichment scores >4 , false discovery rates $<10^{-2}$ for the downregulated DEGs were considered to be significantly enriched. STRING database V.11.5²⁰ was used to investigate known and predicted interactions of the proteins encoded by the DEGs. Both direct (physical) and indirect (functional) interactions were considered setting high confidence (0.700) as the minimum required interaction score. K-means clustering was applied to partition upregulated

DEGs into three networks. Enrichr software²¹ was used to identify transcription modules.

Real-time PCR

62.5 ng of RNAs were reverse transcribed with the PrimeScrip RT Reagent Kit with gDNA Eraser (Takara) in a total volume of 20 μ L. cDNA was diluted twofold with nuclease-free water and 1 μ L cDNA was amplified in a total volume of 25 μ L using the SYBR Premix Ex Taq II (Tli RNaseH Plus) containing the ROX Reference Dye (Takara) and the following QuantiTect primer assays (Qiagen): CCL18 (QT00024066), TNFRSF7/CD27 (QT00044079), TNFRSF4/OX40 (QT00022428), TNFRSF9/4-1BB (QT00043022), PTPRC (alias CD45, QT00028791). POLR2A (QT00033264) was used as a reference to normalise gene expression data.

RESULTS

DEGs in TABs

The expression of 770 genes was investigated with the Nanostring nCounter PanCancer Immune Profiling Panel in 46 TABs with TMI, 7 TABs with ILA and 7 normal TABs without inflammation. Four samples with TMI did not pass the quality controls of the assay, thus were excluded. All the patients with TMI and patients with normal TABs were naïve from therapy at the time of TABs, while 4/7 patients with ILA were receiving glucocorticoids at the time of TABs. Specifically, patient#36 was taking 18.75 mg/day prednisone for 11 days; patient#37 was taking 60 mg/day prednisone for 4 days; patient#39 was taking 50 mg/day prednisone for 14 days and patient#40 was taking 50 mg/day prednisone for 30 days. The diagnosis of GCA in patients with ILA was confirmed by other tests. Of the seven patients with ILA, three patients had temporal artery intima-media thickness ≥ 0.4 mm at colour Doppler ultrasonography, three patients had evidence of large vessel GCA at imaging (two patients at positron emission tomography/computed tomography (PET/CT) and one patient at CT angiography); one patient did not undergo temporal artery or large vessel imaging, but presented with a clinical picture highly suggestive of GCA characterised by bilateral anterior ischaemic optic neuropathy preceded by new-onset headache, jaw claudication and elevation of inflammatory markers, with thickened, nodular and tender temporal arteries at physical examination. The final diagnoses of the patients with normal TABs were polymyalgia rheumatica (two patients), prostate carcinoma, headache with postherpetic neuralgia, non-arteritic anterior ischaemic optic neuropathy, chronic ischaemic heart disease and mitral valve disease, fibromyalgia. Patients and control clinical characteristics at TABs are reported in table 1. The distributions of males and females among the groups were not statistically different applying the Fisher's exact test. Moreover, patients in the three groups had similar ages applying the Kruskal-Wallis test. Age and

Table 1 Clinical characteristics of the patients with and without GCA

Demographic, clinical and laboratory characteristics	TMI	ILA	NEG
Number	42	7	7
Age at disease onset, median (IQR), years	78 (69–80)	70 (65–82)	75 (68–78)
Males/females, n	9/33	3/4	4/3
Any cranial symptoms*, n (%)	41 (98)	7 (100)	5 (71)
Any visual symptoms†, n (%)	8 (19)	3 (43)	3 (43)
Systemic signs/symptoms‡, n (%)	31 (74)	4 (57)	3 (43)
Polymyalgia rheumatica, n (%)	13 (31)	1 (14)	2 (29)
ESR, median (IQR), mm/hour	90 (74–116)	38 (7–102)	30 (24–44)
CRP, median (IQR), mg/dL§	8.35 (3.83–15.70)	6.73 (1.63–13.18)	1.06 (0.22–1.41)
Prednisone at TABs, n (%)	0 (0)	4 (57)	0 (0)

*At least one of the following: headache, scalp tenderness, jaw claudication.

†At least one of the following: sight loss, diplopia, amaurosis fugax.

‡At least one of the following: fever, fatigue, anorexia, weight loss of at least 4 kg.

§Upper limit of the normal reference range=0.5 mg/dL.

CRP, C reactive protein; ESR, erythrocyte sedimentation rate; GCA, giant cell arteritis; ILA, inflammation limited to adventitia; NEG, normal temporal artery biopsies without inflammation from patients without GCA; TAB, temporal artery biopsy; TMI, transmural inflammation.

sex were thus not confounding factors that needed to be introduced as covariates in the analyses.

322 genes were detected in all the samples (online supplemental table 1), while 55 genes were not detected in $\geq 98\%$ of the samples (online supplemental table 1). Specifically, mRNAs of some cytokines were not detected: *IFNA1*, *IFNA8*, *IFNA17*, *IFNB1*, *IFNL2*, *IL-2*, *IL-3*, *IL-5*, *IL-9*, *IL-11*, *IL-12B*, *IL-17A*, *IL-19*, *IL-22*, *IL-25* and cancer-associated antigens.

After normalisation of raw gene counts over the positive and the negative control probes as well as 18 house-keeper genes included in the assay, we identified the DEGs between the groups of samples. We considered significant DEGs those with absolute fold changes between the geometric means of the normalised gene counts >2.0 and Benjamini-Yekutieli adjusted p values <0.05 . Based on such cut-offs, TABs with TMI showed 256 upregulated and 31 downregulated genes compared with normal TABs. TABs with TMI showed 187 upregulated and 26 downregulated genes compared with TABs with ILA (figure 1). TABs with ILA revealed a gene expression profile similar to normal TABs: 38 genes reached fold changes >2.0 , but p values did not maintain statistical significance after correction for multiple testing. Table 2 lists the top-10 deregulated genes according to fold changes in the different comparisons. Online supplemental table 1 lists the 770 genes with fold changes and respective p values, geometric means of the normalised expression levels with SD and numbers of detectable samples in the three groups (ie, histological types of TABs).

We then searched for genes resulting detectable in the majority of the inflamed TABs but not detectable in any normal TABs: 34 genes were present in ≥ 35 TABs with TMI, while they were absent in all the normal TABs (table 3) (Fisher's exact test $p<0.0001$). *CD27* was present in 6 TABs with ILA, while it was absent in all the normal

TABs (Fisher's exact test $p=0.0047$). *IL21R*, *IL1RN*, *CXCL10*, *ICOS* were present in five TABs with ILA, while they were absent in all the normal TABs (Fisher's exact test $p=0.021$).

By means of Venn diagrams, we identified the genes deregulated in the same way in the two-group (histology) comparisons. All the genes upregulated in ILA versus normal TABs were also upregulated in TMI versus normal TABs. 148 genes were upregulated in TMI both versus ILA and normal TABs. *GZMA*, *GZMK*, *FCGR2A*, *MRC1*, *CD163*, *ISG20*, *CXCL10* were upregulated in ILA versus normal TABs and were equally expressed in ILA versus TMI. 35 genes were upregulated in ILA versus normal TABs, and then further increased in TMI versus both ILA and normal TABs: *CCL18*, *CXCL9*, *CIQA*, *ITGAX*, *LTB*, *ITGB2*, *IKBKE*, *IL21R*, *JAK3*, *LCPI*, *CTSS*, *HCK*, *LAIR2*, *FCGR3A*, *CD53*, *CD84*, *CCL3L1*, *SYK*, *IL7R*, *IL2RG*, *IRF4*, *PTPRC/CD45*, *IL1RN*, *HLA-DMB*, *CD27*, *TLR1*, *TLR2*, *C3AR1*, *MSR1*, *F13A1*, *CRI*, *SELPLG*, *LY96*, *NCF4*, *ICOS* (online supplemental figure 1A). 19 genes resulted downregulated in TMI both versus ILA and normal TABs: *ABL1*, *NOL7*, *TOLLIP*, *ITGB3*, *PDGFRB*, *FEZ1*, *AKT3*, *CCL14*, *LRRN3*, *ITGA1*, *IGF1R*, *JAM3*, *CFD*, *CX3CL1*, *CYFIP2*, *MFG8*, *TGFB2*, *RRAD*, *MCAM* (online supplemental figure 1B).

Glucocorticoids can influence gene expression and might have impacted the transcriptome of TABs with ILA. We thus compared the normalised expression of the 770 genes between TABs with ILA from patients naive from therapy ($n=3$) and taking glucocorticoids ($n=4$) by applying the Student's t-test. We did not find any DEGs considering twofold changes and adjusted p values <0.05 .

Unsupervised clustering of the samples

Unsupervised hierarchical clustering based on the normalised gene expression of the 770 genes revealed

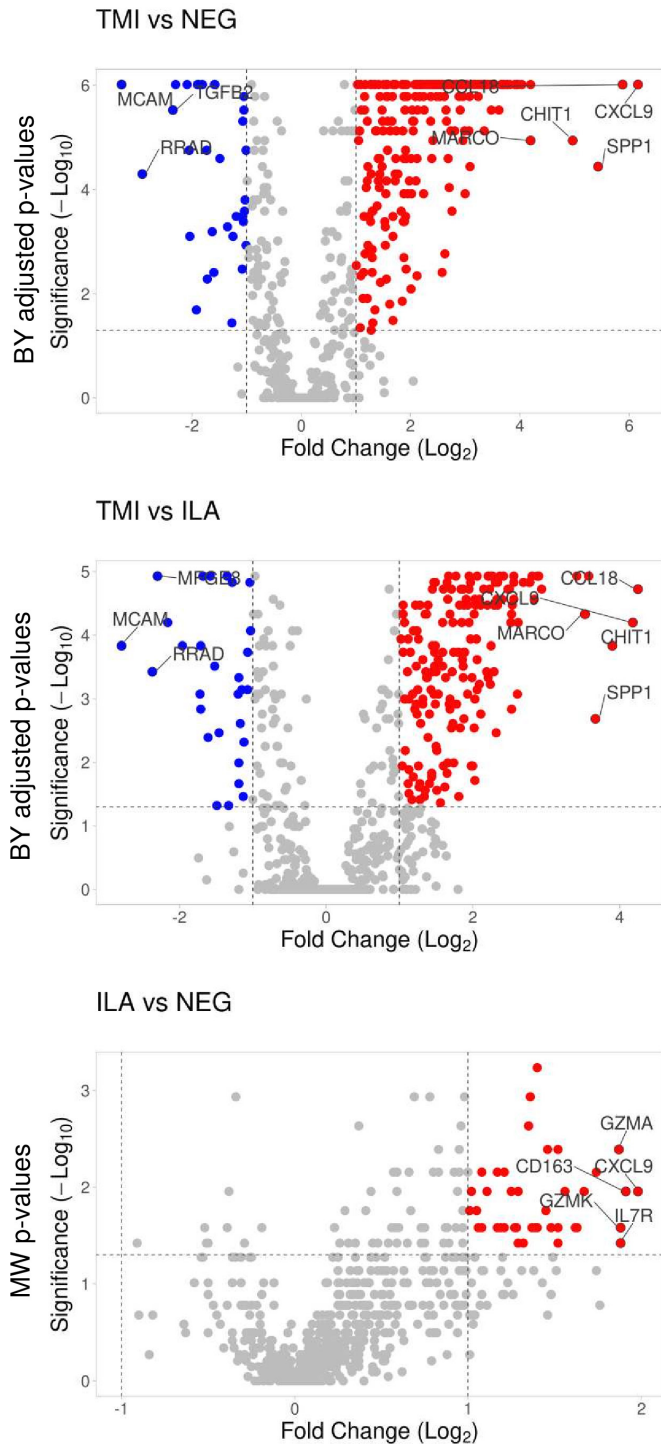


Figure 1 Visualisation of the differentially expressed genes between the histological patterns of inflammation in TABs. Volcano plots show \log_2 (fold changes of normalised gene counts) in the x-axis; $-\log_{10}$ (p values) in the y-axis. Red dots represent the upregulated genes with >2 fold changes and p values <0.05 . Blue dots represent the downregulated genes with <-2 fold changes and p values <0.05 . Benjamini-Yekutieli (BY) adjusted p values are shown for TMI versus NEG and TMI versus ILA. Uncorrected p values resulting from Mann-Whitney (MW) test are shown for ILA versus NEG. ILA, inflammation limited to adventitia; NEG, TABs without inflammation; TABs, temporal artery biopsies; TMI, transmural inflammation.

two groups of samples: the first group contained all the normal TABs, TABs with ILA and TMI#52, while the second group contained 41/42 TABs with TMI (figure 2A). Indeed, five of the seven ILA samples plus TMI#52 formed a separate subgroup. A subset of genes belonging to the TNF superfamily allowed to clearly cluster TABs with TMI from those with ILA and normal TABs (figure 2B). Principal component analysis revealed three groups of samples: the first group contained all the normal TABs plus two TABs with ILA; the second group contained five TABs with ILA plus TMI#52; the third group contained all the remaining TABs with TMI (figure 2C). The two ILA samples which were located nearer to the normal TABs were from patients naive from therapy.

Gene-enriched pathways in inflamed TABs and encoded-protein interactions

Using the DAVID software, we gained insight into the potential biological meaning of the DEGs. Functional annotation clustering highlighted the following pathways as enriched with upregulated DEGs between TMI and normal TABs (enrichment score >8 , false discovery rate $<10^{-6}$): toll-like receptor TLR2, TLR6:TLR2, TLR1:TLR2, TLR7/8, TLR9 cascade, MyD88 cascade initiated on plasma membrane and endosome, chemokine receptors bind chemokines, signalling by G-protein-coupled receptors, PD-1 signalling, translocation of ZAP-70 to immunological synapse, phosphorylation of CD3 and TCR zeta chains, TRAF6 mediated induction of NF- κ B and MAP kinases, lymphocyte, monocyte, eosinophil chemotaxis, cellular response to IL-1, cellular response to TNF. Functional annotation clustering highlighted the following pathways as enriched with downregulated DEGs between TMI and normal TABs (enrichment score >4 , false discovery rate $<10^{-2}$): platelet degranulation, cell-matrix adhesion, integrin-mediated signalling pathway.

Using the Enrichr software, transcription modules, we identified that upregulated genes could be linked to RELA, NFKB1, SPI1, STAT1 transcriptional regulatory networks (adjusted $p < 10^{-19}$, TRRUST Transcription Factors 2019). In addition, they could be regulated by miR-146a-5p (adjusted $p = 0.0007$, miRTarBase 2017).

Using the STRING software, we looked for interactions among DEG encoded proteins and set the formation of three networks based on k-means clustering. The first cluster identified in the genes upregulated in TMI reflects the immune cell infiltrate present in the arteries and associated crosstalk molecules (online supplemental figure 2A). A second cluster links TNF α , IL1 β , IL-18, TLRs and chemokines (online supplemental figure 2B). The third cluster is focused on interferon regulatory factors (IRF) genes, HLA-A/B/C, SH2D1A (online supplemental figure 2C). Focusing on downregulated genes in TABs with TMI, a network centred on ITGB3 appeared (online supplemental figure 2D).

Table 2 Top-10 deregulated genes in TABs

TMI versus NEG			TMI versus ILA			ILA versus NEG		
Gene	FC	BY P value	Gene	FC	BY P value	Gene	FC	MW p value*
CXCL9	71.4	0.000001	CCL18	19.0	0.000019	CXCL9	3.9	0.011072
CCL18	58.9	0.000001	CXCL9	18.1	0.000063	CD163	3.8	0.011072
SPP1	43.1	0.000036	CHIT1	14.9	0.000146	IL7R	3.7	0.037879
CHIT1	31.4	0.000011	SPP1	12.7	0.002058	GZMK	3.7	0.026224
MARCO	18.4	0.000011	MARCO	11.6	0.000047	GZMA	3.6	0.004079
ITGB2	16.5	0.000001	CCL19	10.7	0.000012	IL2RG	3.3	0.006993
C1QB	15.7	0.000001	CYBB	7.7	0.000019	CR1	3.2	0.011072
LTB	15.5	0.000001	IDO1	7.4	0.000012	CCL18	3.1	0.026224
ITGAX	15.3	0.000001	CD74	7.4	0.000012	CD53	3.1	0.026224
CYBB	15.0	0.000001	IL2RB	7.3	0.000012	FCGR3A	2.9	0.011072
MCAM	-9.8	0.000001	MCAM	-6.9	0.000146			
RRAD	-7.5	0.000050	RRAD	-5.2	0.000374			
TGFB2	-5.1	0.000003	MFGE8	-4.9	0.000012			
MFGE8	-4.9	0.000001	CX3CL1	-4.5	0.000063			
CYFIP2	-4.3	0.000001	CYFIP2	-3.9	0.000146			
CX3CL1	-4.2	0.000018	PDGFRB	-3.3	0.000842			
CFD	-4.1	0.000790	TGFB2	-3.3	0.001453			
PPBP	-3.8	0.020432	LRRN3	-3.3	0.000146			
JAM3	-3.7	0.000001	JAM3	-3.2	0.000012			
IGF1R	-3.7	0.000001	CCL14	-3.1	0.004051			

*Uncorrected p values resulting from Mann-Whitney test.

BY, Benjamini-Yekutieli ; FC, fold changes; ILA, inflammation limited to adventitia; NEG, normal temporal artery biopsies without inflammation from patients without GCA; TABs, temporal artery biopsies; TMI, transmural inflammation.

Expression of genes reflecting infiltrating immune cell types

To determine which types of infiltrating immune cells were present in the TABs we searched for specific markers. *CD45/PTPRC*, mirroring total infiltrating leukocytes, was more expressed in TMI. In particular, *CD45* normalised counts higher than 293 separated TMI and normal TABs with 100% sensitivity and specificity. TABs with ILA revealed to be heterogeneous: five samples had *CD45* values ≥ 293 while two samples had *CD45* values similar to normal TABs (ILA#41 and ILA#59). These samples were from patients naïve from therapy. Markers of monocytes/macrophages and CD4+T lymphocytes were highly expressed in TMI. *CD19*, marker of B lymphocytes, was more expressed in TABs with TMI while the expression of other markers of B lymphocytes (*CD20*, *BLK*, *CD269*) was heterogeneous in TMI. *DC-SIGN*, reflecting DCs, was higher in 86% of the TABs with TMI. Markers of granulocytes and NK cells were comparable among the samples (figure 3).

Comparison of Nanostring nCounter gene expression data with published DNA methylation data in TABs

To determine if the transcription of some DEGs between TABs with TMI and normal TABs might be controlled by DNA methylation, we compared the DEGs herein

reported with the list of significantly differentially methylated CpG sites in inflamed TABs reported by Coit *et al* in online supplemental material of the manuscript published in *Annals of the Rheumatic Diseases* (thresholds: p values <0.05 and $\Delta\beta >0.20$).¹⁵ We realised that 118 genes were annotated with both hypomethylated and hypermethylated CpG sites.¹⁵ We decided to be stringent including in the comparison exclusively the genes that were annotated with hypomethylated or hypermethylated CpGs. Otherwise, it would have been necessary to calculate a resulting DNA methylation value for each gene. 85 out of the 260 upregulated genes in TABs with TMI had reported hypomethylated CpG sites. 11 out of the 31 downregulated genes in TABs with TMI had reported hypermethylated CpG sites. Seven out of the 260 upregulated genes in TABs with TMI had reported hypermethylated CpG sites (online supplemental table 2).

Comparison of Nanostring nCounter gene expression data with published RNA sequencing data in TABs

To date, there is only one published manuscript on high throughput gene expression profile in whole TABs from patients with and without GCA.¹⁴ Authors compared varicella zoster virus (VZV) antigen-positive versus antigen-negative areas from control TABs and inflamed TABs

Table 3 Genes detected in TABs with TMI but not detected in normal TABs

Gene	TMI (n=42)	ILA (n=7)	NEG (n=7)
CCR7	42	2	0
TNFRSF7/CD27	42	6	0
CD86	42	1	0
CTLA4	42	4	0
CXCR3	42	4	0
CXCR6	42	4	0
IL21R	42	5	0
SLAMF6	42	3	0
SLAMF7	42	4	0
TNFRSF4/OX40	42	1	0
TNFRSF9/4-1BB	42	1	0
CD2	41	3	0
CD6	41	2	0
CD80	41	2	0
FCGR1A	41	1	0
IL1RN	41	5	0
SH2D1A	41	3	0
SLAMF1	41	2	0
TNFSF15	41	1	0
CXCL13	40	3	0
LAG3	40	4	0
TLR7	40	4	0
CD28	39	3	0
LAMP3	39	1	0
BID	38	3	0
CXCL10	38	5	0
ICOS	38	5	0
STAT4	38	2	0
EBI3	37	0	0
GZMM	37	4	0
TNFSF8	37	2	0
CCL22	36	1	0
FUT7	36	2	0
BLNK	35	1	0

The numbers of samples in which the transcripts were detected are shown.

ILA, inflammation limited to adventitia; NEG, normal temporal artery biopsies without inflammation from patients without GCA; TABs, temporal artery biopsies; TMI, transmural inflammation.

by TempO-Seq-targeted RNA sequencing. They did not investigate DEGs between inflamed TABs and normal TABs, without splitting in VZV-positive and VZV-negative areas. Therefore, to compare our data with Bubak *et al.*'s data, we first merged the list of DEGs between GCA/VZV-positive and control/VZV-negative TABs with

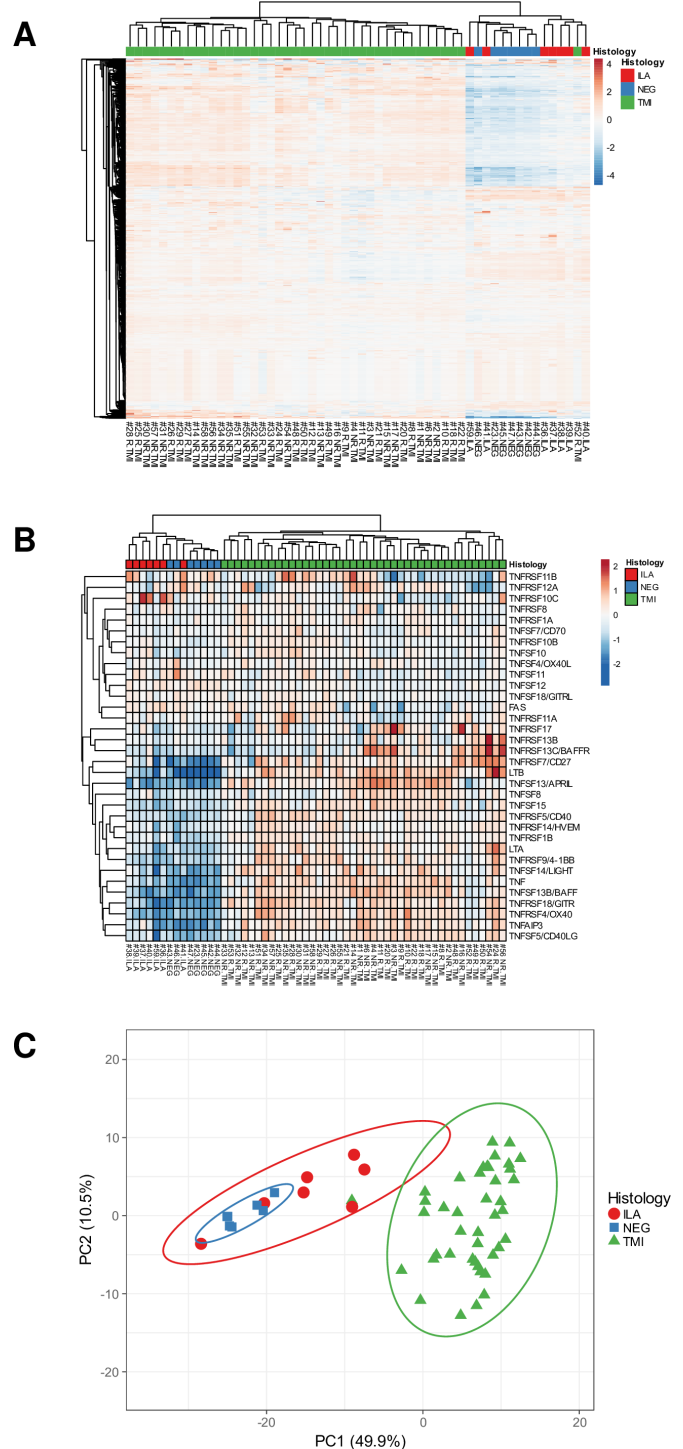
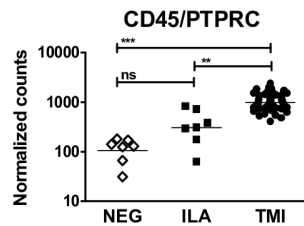


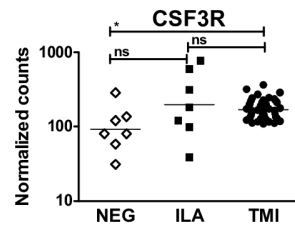
Figure 2 Unsupervised clustering of the samples. (A) Hierarchical clustering using the normalised expression of the 770 genes. (B) Hierarchical clustering using the subset of the TNF superfamily genes. (C) Principal component (PC) analysis using the normalised expression of the 770 genes. The x-axis and y-axis show principal component 1 and principal component 2. N=56 samples. ILA, inflammation limited to adventitia; NEG, TABs without inflammation; TMI, transmural inflammation.

that between GCA/VZV-negative and control/VZV-negative TABs reported in online supplemental materials by Bubak *et al.*¹⁴ We then applied a twofold change threshold so that the data could be compared with the

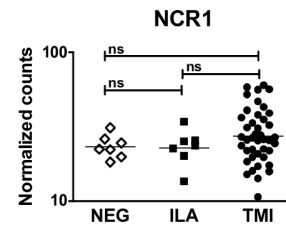
Leukocytes



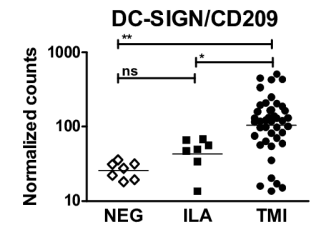
Granulocytes



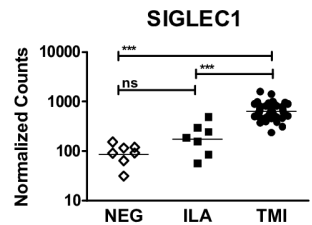
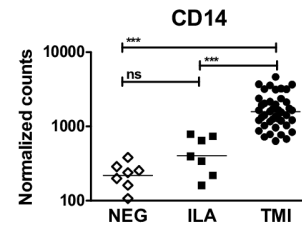
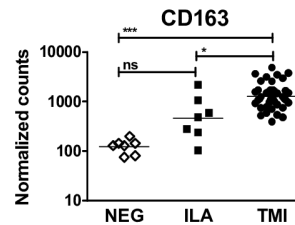
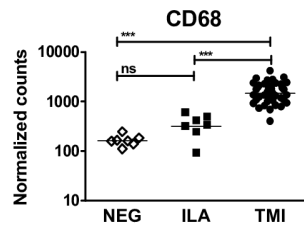
NK cells



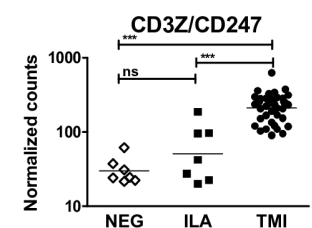
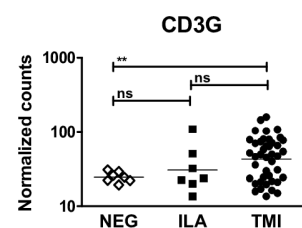
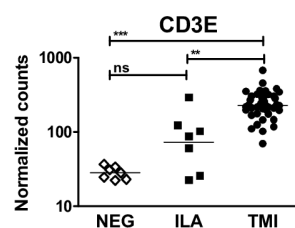
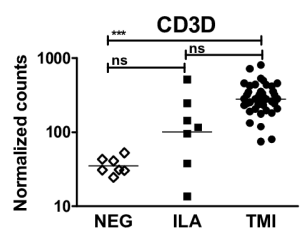
DC cells



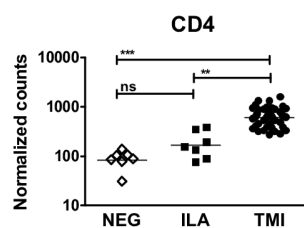
Macrophages



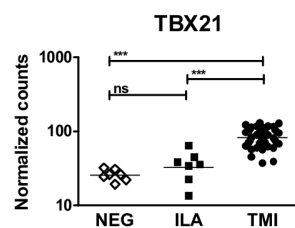
T lymphocytes



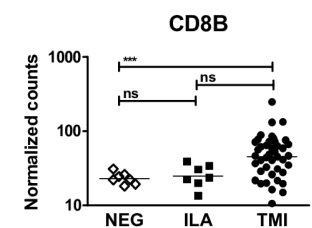
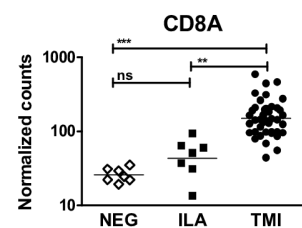
T helper lymphocytes



T helper 1



Cytotoxic T lymphocytes



B lymphocytes

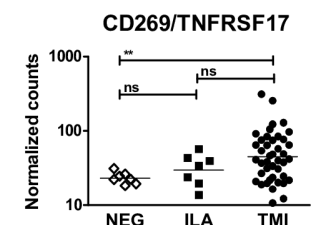
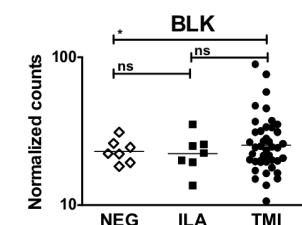
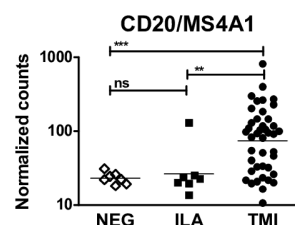
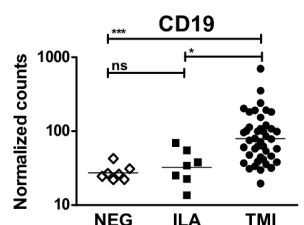


Figure 3 Characterisation of the immune cell infiltrate in temporal artery biopsies. Normalised expression levels of transcripts reflecting T and B lymphocytes, macrophages, granulocytes, natural killer (NK) cells and dendritic cells (DCs), are shown in the group of samples. Lines indicate geometric means. Expression levels in the group of samples were compared with Kruskal-Wallis test with Dunn's post-test, except for CD3G, CD8B, CD20, BLK, CD269 whose expressions were compared with Fisher's exact test. * $p < 0.05$; ** $p < 0.01$; *** $p < 0.001$. ILA, inflammation limited to adventitia; NEG, TABs without inflammation; TMI, transmural inflammation.

herein reported ones. 113 genes resulted similarly upregulated and 6 genes resulted similarly downregulated in TABs with TMI (online supplemental table 3).

Validation of some DEGs

We confirmed the deregulation of some novel genes using a validation cohort ($n=7$ snap-frozen TABs of each

histological pattern) and a validation method (real-time PCR). The characteristics of the validation cohort of patients are reported in online supplemental table 4. We selected *CCL18*, the top upregulated gene in TMI and three genes belonging to TNF receptor superfamily which were detected in all the TABs with TMI and not detected in normal TABs: *TNFRSF7/CD27*, *TNFRSF9/4-1BB*, *TNFRSF4/OX40*.

CCL18 was confirmed to be upregulated in TMI versus normal TABs and TMI versus ILA. *TNFRSF7/CD27* was confirmed to be more frequently detected in TABs with TMI and ILA, while it was undetectable in normal TABs. Moreover, it was expressed at higher levels in TMI versus ILA. *TNFRSF9/4-1BB* was confirmed to be positive in all the TABs with TMI, while it was undetectable in normal TABs. Moreover, it was expressed at higher levels in TMI versus ILA and detected in 4/7 TABs with ILA. *TNFRSF4/OX40* was detected in all the TABs with TMI and ILA and in 6/7 normal TABs, indicating that real-time PCR was more sensitive than Nanostring nCounter for this gene. *OX40* was confirmed to be upregulated in TMI both versus ILA and normal TABs (online supplemental figure 3).

DISCUSSION

Expression profiling of 770 genes in TABs highlighted pathways deregulated in GCA that might play a role in the pathogenesis of this large vessel vasculitis and shed some light on ILA and TMI histological patterns of inflammation. TABs with TMI showed many DEGs versus normal TABs from patients without GCA, while ILA showed few potential genes with increased expression. This finding is partly in line with the results reported by Parreau *et al* using the NanoString GeoMx Digital Spatial Profiler technology.¹³ They followed a different study design. Instead of analysing TABs with different patterns of inflammation (ie, different disease phases or different disease subsets), they analysed gene expression in selected regions of interest from the adventitial, medial and intimal layers and perivascular adipose tissue from TABs with TMI. They found the highest numbers of DEGs in the media and intima while few genes were deregulated in the adventitia. *CD74*, the top upregulated gene between GCA and control specimens,¹³ resulted significant upregulated also in our samples with TMI but not in ILA.

Different gene expression profiles emerged (1) some genes upregulated in ILA versus normal TABs were equally expressed between TMI and ILA; (2) some genes upregulated in ILA versus normal TABs were further upregulated in TMI versus ILA and (3) some genes were upregulated or downregulated in TMI both versus normal TABs and ILA and showed comparable expression between ILA and normal TABs. The first ones might play a role mainly in the early phases of the disease; the second ones might be involved in both early and late

phases; the third ones might have a main role in late phases.

The few promising genes upregulated in ILA versus normal TABs were also upregulated in TMI versus normal TABs. This suggests that ILA might represent early phases of the disease, which can progress towards TMI if further hits occur. We did not find any DEGs between TABs with ILA from patients with and without therapy, which might indicate that glucocorticoids were not the reason for the lack of ILA-specific DEGs and the similarity between the transcriptome of ILA and normal TABs. We are aware that such a comparison is explorative due to the small sample size. Therefore, it cannot yet be ruled out that ILA harbours peculiar molecular characteristics.

The comparison between our results and those obtained by Bubak *et al* using RNA sequencing¹⁴ aimed to identify genes reported as deregulated in TABs from GCA patients across two different transcriptomic analyses in independent cohorts. We think that the genes listed in online supplemental table 3 might, therefore, be considered somehow already validated as deregulated in TABs with TMI, at mRNA level. The comparison between our results and those obtained by Coit *et al* with DNA methylation¹⁵ was used to identify those genes which might be epigenetically regulated, that is, upregulated or downregulated transcripts with reported hypomethylated or hypermethylated CpGs in TABs from GCA patients. Since the one-way gene-silencing role of DNA hypermethylation is now being questioned in particular biological contexts, we listed also the upregulated transcripts with reported hypermethylated CpGs. We are aware that this comparison has some limits (eg, data were obtained from independent cohorts/samples; inclusion only of genes with hypomethylated or hypermethylated CpGs), however, we think that it can provide some rational starting data for future investigations.

Genes belonging to TNF superfamily (ligands and receptors) characterised TMI. They encode type II transmembrane proteins which contain the TNF homology domain. Such proteins can also be released by proteolytic cleavage, acting as soluble mediators. TNF superfamily members have various activities, tuning the immune system and regulating angiogenesis, B cell development, proliferation and differentiation, induction of apoptosis. Interestingly, six TNF receptor superfamily members overexpressed in inflamed TABs are stimulatory immune checkpoint molecules: *CD27/TNFRSF7*, *OX40/TNFRSF4*, *4-1BB/TNFRSF9*, *GITR/TNFRSF18*, *CD40/TNFRSF5* and its ligand *CD40L/TNFSF5*. We validated the overexpression of *CD27/TNFRSF7*, *OX40/TNFRSF4*, *4-1BB/TNFRSF9*. In addition, other stimulatory immune checkpoint molecules emerged upregulated in inflamed TABs: *CD2*, *CD6*, *ICOS*, *CD28* with its two ligands *CD80* and *CD86*. Such stimulatory signals can prime naïve T cells, promote Th1 polarisation, T follicular helper differentiation, enhance proliferation and survival of effector T cells, formation of memory T cells. Upregulation of *CD40/CD40L* can lead to B cell activation and has been previously reported in

TABs by Coit *et al.*¹⁵ CD28-associated pathways have been proven to have a role in GCA. Blocking CD28 in human artery-mouse chimaeras decreased tissue-infiltrating T cells, the ability to use glucose by T cells and to produce IFN γ and IL-21, tissue-resident memory T cells, intimal thickness and adventitial microvessels.²² CD86 has been found expressed by specific DC subsets and some endothelial cells in inflamed TABs while it has been undetectable in normal TABs, indicating the presence of antigen presentation and T cell activation in GCA.²³

Besides stimulatory immune checkpoint, inhibitory immune checkpoint genes emerged also enhanced in TABs with TMI: *CTLA4*, *TIGIT*, *CD96*, *LAG3*, *BTLA*, *HVEM*/*TNFRSF14*, *IDO1*, *PD-L1/CD274*, *PD-L2/PDCD1LG2*. This would be unexpected in autoimmune and inflammatory diseases where immune system is activated but can be explained hypothesising the induction of feedback mechanisms that attempt to shut down inflammation. In addition, it can be explained by a defective expression of the receptor counterpart, as demonstrated by Weyand *et al.*⁴ for the CD155-CD96 immune checkpoint.²⁴ *CTLA4* pathway seems functional in GCA because some patients with metastatic melanoma treated with Ipilimumab, a drug which inhibits *CTLA4*, developed GCA.²⁵ *CTLA4* has been detected in GCA aortic sections, particularly expressed by FoxP3+CD4+ lymphocytes (i.g. Tregs).²⁶ Abatacept, which mimics *CTLA4* activities, leads to weak benefits in patients with GCA,²⁷ which suggests that this pathway is saturated in vivo. Data on the expression of *PD-L1/PD-1* in inflamed TABs are controversial. Weyand *et al.*⁴ reported low expression of *PD-L1* with enrichment of *PD-1* transcripts in inflamed TABs compared with normal TABs, suggesting inefficiency of the inhibitory PD-1/PD-L1 immune checkpoint in GCA.²⁸ Instead, Hid Cadena *et al.* reported increased PD-L1-expressing cells in inflamed TABs.²⁹ We detected an increased expression of both *PD-L1* and *PD-L2* in TABs with TMI, and *PD-1* expression in 64% of the TABs. PD-1/PD-L1 pathway is likely involved in GCA pathogenesis since the administration of an inhibitor of PD-1 exacerbated arterial inflammation and remodelling in human artery-mouse chimaeras,²⁸ and GCA occurred in a patient treated with the PD-1 inhibitor nivolumab.³⁰

Several genes encoding chemokines and chemokine receptors emerged significantly upregulated in inflamed TABs. Chemokines drive the migration of cells during homeostatic and inflammatory conditions. In particular, the following genes encoding both the ligand and the receptor were upregulated: *CXCL9*, *CXCL10*, *CXCL11/CXCR3*, *CXCL16/CXCR6*, *CCL2/CCR2*, *CCL3*, *CCL4*, *CCL5/CCR5*, *CCL19/CCR7*. In addition, genes encoding *CCL22* and *CXCL13/BLC* were detected only in inflamed TABs and *CCL18* was among the top upregulated genes. Interestingly, the loci for *CXCR3*, *CXCR6*, *CCR2*, *CCR5*, *CCR7*, *CCL18*, *CCL22* have been reported hypomethylated in inflamed TABs,¹⁵ which could support their upregulation assuming that hypomethylation can lead to gene overexpression. The deregulated chemokines can favour

the recruitment of monocytes, T lymphocytes, memory T cells, NK, NKT and DCs to the sites of inflammation and B cells to lymphoid tissues. Overexpression of *CXCL9*, *CXCL10*, *CXCL11/CXCR3*, *CXCL13/BLC*, *CCL18*, *CCL19/CCR7*, *CCL2/CCR2*, *CCR5* in inflamed TABs from GCA patients has been reported by other authors by means of gene expression and/or immunohistochemistry analysis,^{7 23 31–34} while overexpression of *CXCL16/CXCR6* and *CCL22* is novel. Development of agents to block chemokine pathways in the arteries may provide new ways to treat GCA.

Another cluster of genes which resulted upregulated in inflamed TABs encodes TLRs (ie, *TLR1*, *TLR2*, *TLR4*, *TLR6*, *TLR7*, *TLR8*). TLRs are transmembrane proteins expressed by cells of the immune system and tissue cells which link innate and adaptive immunity and act as a first line of defence as pattern recognition receptors. It has been demonstrated that TLR binding can activate DCs and break self-tolerance in GCA, supporting a model in which TLR ligands may initiate vessel wall inflammation.³⁵ Specifically, *TLR4* triggering has been shown to induce TMI, while *TLR5* triggering has been shown to promote adventitial perivasculitis.³⁶ Functional data on other TLRs are lacking.

JAKs are intracellular tyrosine kinases that transduce signals from cytokine receptors and ultimately act through STAT proteins. Several drugs have been developed which inhibit specific JAKs or are pan-JAK inhibitors. Since JAKs are hub proteins which control proinflammatory and protective immune responses, it is important to define which JAKs should be specifically targeted in each immune-mediated disease.³⁷ The Nanostring nCounter gene profiling showed an increased expression of *JAK3*, *STAT1*, *STAT4* pointing to these targets as the most promising in GCA. Data on *JAK3*, *STAT1* and *STAT4* upregulation in TMI are consistent with published data,^{7 14 38} and *STAT1* and *STAT4* overexpression might be driven by DNA hypomethylation.¹⁵ The JAK1/3 inhibitor Tofacitinib decreased arterial inflammation and remodelling in human artery-mouse chimaeras.³⁸ The JAK1/2 inhibitor Baricitinib showed some efficacy in patients with relapsing GCA.³⁹

To date, expression levels of several cytokines have been investigated in GCA,⁴ while less attention has been paid to the respective receptors. Coupling cytokine and cytokine-receptor gene expression revealed the potential activation of IL-1 β , IL-10, IL-15, IL-16, IL-18, IL-21, IL-32, TNF α , GM-CSF, M-CSF signalling pathways in GCA. IL21/IL-21R expression has been demonstrated in inflamed TABs¹⁵ and it has been suggested that IL-21 may modulate Th1, Th17 and Treg responses in GCA.⁴⁰ GM-CSF and M-CSF have been detected in inflamed TABs, where they can favour the development of specific macrophage subsets.⁴¹ Blocking GM-CSFR with Mavrilimumab in ex vivo cultured arteries from patients with GCA reduced infiltrating immune cells, proinflammatory cytokine production and neoangiogenesis.⁸ Moreover, Mavrilimumab appeared to be effective in vivo, reducing

flare occurrence in patients with GCA,⁴² thus supporting a pathogenic role for GM-CSF pathway. IL-32 has been detected at mRNA and protein levels in inflamed TABs from patients with GCA, expressed by vascular smooth muscle cells and neovessels.⁴³ TNF α has been detected to be produced by giant cells, macrophages and endothelial cells in TABs.⁴⁴ However, biological agents anti-TNF α revealed to be ineffective in GCA patients.^{45 46} IL-1 β and IL-18 belong to the IL-1 family of cytokines. IL-1 β has been reported in inflamed TABs. Blocking IL-1 β with the administration of Anakinra was revealed to be effective in case reports and case series of patients with refractory GCA,^{47 48} but randomised controlled trials and in vitro studies are needed to prove a pathogenic role for IL-1 β in GCA. To be noted, we found that the interleukin-1 receptor antagonist (*IL1RN*), the endogenous gene that Anakinra mimics, is expressed in inflamed TABs with TMI and ILA but is not expressed in normal TABs. Therefore, we suggest that the direct inhibition of IL-1 β would be more rationale than the antagonism of its receptor.

Regarding the immunological pathways most studied to date in GCA, mRNAs of *IL-6*, *IFN γ* and their receptors did not result significantly differentially expressed between inflamed and normal TABs; mRNA of *IL-17RA* resulted overexpressed but mRNAs of the ligands (ie, IL-17 cytokines) were not detected; similarly mRNA of *IL-12RB1* resulted overexpressed but mRNAs of the interactors (*IL-12A*, *IL-12B*, *IL-23A*, *IL-12RB*, *IL-23R*) were not detected or scarcely detected.

Novel genes emerged increased in TABs with TMI: complement molecules (*C1QA*, *C1QB*, *C2*, *C3AR1*, *CRI*, *C4B*); Fc receptors for IgG antibodies (*FCGR1A*, *FCGR2A*, *FCGR3A*, *FCGR2B*); signalling lymphocytic activation molecules (*SLAMF1*, *SLAMF2*, *SLAMF5*, *SLAMF6*, *SLAMF7*). *C1QA* and *C1QB* were reported upregulated in the intima and media layers of inflamed TABs also by Parreu *et al.*¹³ These data suggest a possible role of the classical complement pathway and of IgG antibodies bound via FCGRs in GCA. SLAM family transmembrane receptors are expressed by several immune cells and have an emerging role in autoimmune diseases (eg, systemic lupus erythematosus and rheumatoid arthritis),^{49 50} immunological disorders and cancers (eg, multiple myeloma). Elotuzumab, an antibody that targets SLAMF7, is used in multiple myeloma.

The analysis of markers of immune cell subsets showed that the degrees of leucocyte infiltration were more variable in ILA than in TMI. Data suggested that glucocorticoids were not the reason for the heterogeneity in CD45 levels in ILA. Since we extracted RNA from several consecutive tissue slices, it could indicate that the ILA pattern is more patchy than the TMI pattern of inflammation. All the TABs with TMI expressed markers of T lymphocytes and macrophages while they were revealed to be heterogeneous regarding the presence of B cells.

The present study has several strengths. We profiled gene expression in a large number of samples with TMI, collected from patients free of glucocorticoids at the time

of TABs, indicating that glucocorticoid treatment did not influence the results of our gene expression analysis. We used an innovative technique for gene expression profiling: the Nanostring nCounter technology, which is suitable for archived FFPE tissues. We investigated gene expression at the tissue level, in TABs, instead of peripheral blood. We identified several DEGs, applying multiple testing corrections, indicating that gene expression differences between TABs with TMI and negative TABs are reliable. The limitations of this study concern the small number of negative TABs and TABs with ILA because it was difficult to obtain sufficient quantity and good-quality RNA from negative TABs and TABs with ILA. We extracted RNA from a larger number of samples but only the ones herein analysed were suitable. Furthermore, due to the lower frequency of the ILA inflammation pattern (7% of all the inflamed TABs), we had to analyse TABs with ILA collected from patients under glucocorticoid therapy. Finally, we analysed a set of genes linked to inflammation and immune cells instead of the whole transcriptome.

In conclusion, we uncovered novel molecules and pathways possibly involved in the pathogenesis of GCA as well as confirmed the deregulation of known ones. TNF superfamily members, immune checkpoints, chemokines, TLRs, JAK3, classic complement molecules, FCGRs and SLAMFs emerged overexpressed. TMI showed a distinct transcriptome compared with normal TABs, while ILA appeared heterogeneous. We speculate that ILA might represent the early phases of the disease. Since parts of the TABs with ILA were collected from patients receiving glucocorticoids, further studies are needed to verify if ILA precedes TMI or is a different subset.

Author affiliations

¹Clinical and Experimental Medicine PhD Program, University of Modena and Reggio Emilia, Modena, Italy

²Unit of Clinical Immunology, Allergy and Advanced Biotechnologies, Azienda Unità Sanitaria Locale - IRCCS di Reggio Emilia, Reggio Emilia, Italy

³Unit of Rheumatology, Azienda Unità Sanitaria Locale - IRCCS di Reggio Emilia, Reggio Emilia, Italy

⁴Surgery, Medicine, Dentistry and Morphological Sciences with Interest in Transplant, Oncology and Regenerative Medicine, University of Modena and Reggio Emilia, Modena, Italy

⁵Unit of Pathology, Azienda Unità Sanitaria Locale - IRCCS di Reggio Emilia, Reggio Emilia, Italy

⁶Unit of Ocular Immunology, Azienda Unità Sanitaria Locale - IRCCS di Reggio Emilia, Reggio Emilia, Italy

⁷Unit of Otolaryngology, Azienda Unità Sanitaria Locale - IRCCS di Reggio Emilia, Reggio Emilia, Italy

⁸Unit of Vascular Surgery, Azienda Unità Sanitaria Locale - IRCCS di Reggio Emilia, Reggio Emilia, Italy

Contributors SC and CS are responsible for the overall content as the guarantor. IF, MB, AR, MN and AB performed the experiments and analysed the data; FM, LB, AC, LC, AG, GM and NP collected tissue and clinical data; AZ contributed to interpret the data; CS contributed to data interpretation, supervision and funding acquisition; SC designed the experiments, analysed and interpreted the data, prepared the original draft of the manuscript, contributed to supervision and funding acquisition. All authors read, reviewed and approved the final manuscript. The corresponding author attests that all listed authors meet authorship criteria and that no others meeting the criteria have been omitted.

Funding This study was funded by Azienda Unità Sanitaria Locale-IRCCS di Reggio Emilia, Reggio Emilia, Italy: 'Bando per la valorizzazione della Ricerca Istituzionale 2019'; Foundation for Research in Rheumatology (FOREUM) 'Call for Research Proposals on Stratified Medicine in Rheumatology 2017' and the competitive call 'Roche Sostiene la Ricerca 2016'.

Disclaimer Funders were not involved in any part of study design, analysis or writing of the manuscript.

Competing interests None declared.

Patient consent for publication Not applicable.

Ethics approval The study was approved by the local Ethics Committee 'Comitato Etico dell'Area Vasta Emilia Nord' on 26 March 2020 (study number 107/2020/OSS/AUSLRE). All reasonable efforts were made to contact the patients to collect informed consent. However, given the retrospective nature of the study, the ethics committee waived the need for informed consent in case it was not possible to contact the patients.

Provenance and peer review Not commissioned; externally peer reviewed.

Data availability statement Data are available on reasonable request. All data relevant to the study are included within the article or uploaded as online supplemental information. Single sample gene expression data will be available on reasonable request to the corresponding author.

Supplemental material This content has been supplied by the author(s). It has not been vetted by BMJ Publishing Group Limited (BMJ) and may not have been peer-reviewed. Any opinions or recommendations discussed are solely those of the author(s) and are not endorsed by BMJ. BMJ disclaims all liability and responsibility arising from any reliance placed on the content. Where the content includes any translated material, BMJ does not warrant the accuracy and reliability of the translations (including but not limited to local regulations, clinical guidelines, terminology, drug names and drug dosages), and is not responsible for any error and/or omissions arising from translation and adaptation or otherwise.

Open access This is an open access article distributed in accordance with the Creative Commons Attribution Non Commercial (CC BY-NC 4.0) license, which permits others to distribute, remix, adapt, build upon this work non-commercially, and license their derivative works on different terms, provided the original work is properly cited, appropriate credit is given, any changes made indicated, and the use is non-commercial. See: <http://creativecommons.org/licenses/by-nc/4.0/>.

ORCID iDs

Martina Bonacini <http://orcid.org/0000-0002-6830-6781>

Francesco Muratore <http://orcid.org/0000-0003-0362-2668>

Stefania Croci <http://orcid.org/0000-0002-8622-0439>

REFERENCES

- Salvarani C, Pipitone N, Versari A, *et al*. Clinical features of polymyalgia rheumatica and giant cell arteritis. *Nat Rev Rheumatol* 2012;8:509–21.
- Cavazza A, Muratore F, Boiardi L, *et al*. Inflamed temporal artery: histologic findings in 354 biopsies, with clinical correlations. *Am J Surg Pathol* 2014;38:1360–70.
- Régent A, Mouthon L. Treatment of Giant Cell Arteritis (GCA). *J Clin Med* 2022;11:1799.
- Weyand CM, Goronzy JJ. Immunology of Giant Cell Arteritis. *Circ Res* 2023;132:238–50.
- Samson M, Corbera-Bellalta M, Audia S, *et al*. Recent advances in our understanding of giant cell arteritis pathogenesis. *Autoimmun Rev* 2017;16:833–44.
- Brack A, Geisler A, Martinez-Taboada VM, *et al*. Giant cell vasculitis is a T cell-dependent disease. *Mol Med* 1997;3:530–43.
- Corbera-Bellalta M, Planas-Rigol E, Lozano E, *et al*. Blocking interferon γ reduces expression of chemokines CXCL9, CXCL10 and CXCL11 and decreases macrophage infiltration in ex vivo cultured arteries from patients with giant cell arteritis. *Ann Rheum Dis* 2016;75:1177–86.
- Corbera-Bellalta M, Alba-Rovira R, Muralidharan S, *et al*. Blocking GM-CSF receptor α with mavrilimumab reduces infiltrating cells, pro-inflammatory markers and neoangiogenesis in ex vivo cultured arteries from patients with giant cell arteritis. *Ann Rheum Dis* 2022;81:524–36.
- Conway R, O'Neill L, McCarthy GM, *et al*. Interleukin 12 and interleukin 23 play key pathogenic roles in inflammatory and proliferative pathways in giant cell arteritis. *Ann Rheum Dis* 2018;77:1815–24.
- Lozano E, Segarra M, García-Martínez A, *et al*. Imatinib mesylate inhibits in vitro and ex vivo biological responses related to vascular occlusion in giant cell arteritis. *Ann Rheum Dis* 2008;67:1581–8.
- Terrades-García N, Cid MC. Pathogenesis of giant-cell arteritis: how targeted therapies are influencing our understanding of the mechanisms involved. *Rheumatology (Oxford)* 2018;57:ii51–62.
- Ciccía F, Macaluso F, Mauro D, *et al*. New insights into the pathogenesis of giant cell arteritis: are they relevant for precision medicine? *Lancet Rheumatol* 2021;3:e874–85.
- Parreau S, Molina E, Dumonteil S, *et al*. Use of high-plex data provides novel insights into the temporal artery processes of giant cell arteritis. *Front Immunol* 2023;14:1237986.
- Bubak AN, Mescher T, Mariani M, *et al*. Targeted RNA Sequencing of Formalin-Fixed, Paraffin-Embedded Temporal Arteries From Giant Cell Arteritis Cases Reveals Viral Signatures. *Neurol Neuroimmunol Neuroinflamm* 2021;8:e0178.
- Coit P, De Lott LB, Nan B, *et al*. DNA methylation analysis of the temporal artery microenvironment in giant cell arteritis. *Ann Rheum Dis* 2016;75:1196–202.
- Croci S, Zerbinì A, Boiardi L, *et al*. MicroRNA markers of inflammation and remodelling in temporal arteries from patients with giant cell arteritis. *Ann Rheum Dis* 2016;75:1527–33.
- Goedhart J, Luijsterburg MS. VolcanoR is a web app for creating, exploring, labeling and sharing volcano plots. *Sci Rep* 2020;10:20560.
- Metsalu T, Vilo J. ClustVis: a web tool for visualizing clustering of multivariate data using Principal Component Analysis and heatmap. *Nucleic Acids Res* 2015;43:W566–70.
- Huang DW, Sherman BT, Lempicki RA. Systematic and integrative analysis of large gene lists using DAVID bioinformatics resources. *Nat Protoc* 2009;4:44–57.
- Szklarczyk D, Gable AL, Nastou KC, *et al*. The STRING database in 2021: customizable protein-protein networks, and functional characterization of user-uploaded gene/measurement sets. *Nucleic Acids Res* 2021;49:D605–12.
- Chen EY, Tan CM, Kou Y, *et al*. Enrichr: interactive and collaborative HTML5 gene list enrichment analysis tool. *BMC Bioinformatics* 2013;14:128.
- Zhang H, Watanabe R, Berry GJ, *et al*. CD28 Signaling Controls Metabolic Fitness of Pathogenic T Cells in Medium and Large Vessel Vasculitis. *J Am Coll Cardiol* 2019;73:1811–23.
- Krupa WM, Dewan M, Jeon M-S, *et al*. Trapping of misdirected dendritic cells in the granulomatous lesions of giant cell arteritis. *Am J Pathol* 2002;161:1815–23.
- Ohtsuki S, Wang C, Watanabe R, *et al*. Deficiency of the CD155-CD96 immune checkpoint controls IL-9 production in giant cell arteritis. *Cell Rep Med* 2023;4:101012.
- Goldstein BL, Gedmintas L, Todd DJ. Drug-associated polymyalgia rheumatica/giant cell arteritis occurring in two patients after treatment with ipilimumab, an antagonist of ctla-4. *Arthritis Rheumatol* 2014;66:768–9.
- Régnier P, Le Joncour A, Maciejewski-Duval A, *et al*. CTLA-4 Pathway Is Instrumental in Giant Cell Arteritis. *Circ Res* 2023;133:298–312.
- Langford CA, Cuthbertson D, Ytterberg SR, *et al*. A Randomized, Double-Blind Trial of Abatacept (CTLA-4Ig) for the Treatment of Giant Cell Arteritis. *Arthritis Rheumatol* 2017;69:837–45.
- Zhang H, Watanabe R, Berry GJ, *et al*. Immunoinhibitory checkpoint deficiency in medium and large vessel vasculitis. *Proc Natl Acad Sci U S A* 2017;114:E970–9.
- Hid Cadena R, Reitsema RD, Huitema MG, *et al*. Decreased Expression of Negative Immune Checkpoint VISTA by CD4+ T Cells Facilitates T Helper 1, T Helper 17, and T Follicular Helper Lineage Differentiation in GCA. *Front Immunol* 2019;10:1638.
- Betrains AE, Blockmans DE. Immune Checkpoint Inhibitor-Associated Polymyalgia Rheumatica/Giant Cell Arteritis Occurring in a Patient After Treatment With Nivolumab. *J Clin Rheumatol* 2021;27:S555–6.
- Brühl H, Vielhauer V, Weiss M, *et al*. Expression of DARC, CXCR3 and CCR5 in giant cell arteritis. *Rheumatology (Oxford)* 2005;44:309–13.
- Ciccía F, Rizzo A, Maugeri R, *et al*. Ectopic expression of CXCL13, BAFF, APRIL and LT- β is associated with artery tertiary lymphoid organs in giant cell arteritis. *Ann Rheum Dis* 2017;76:235–43.
- Samson M, Ly KH, Tournier B, *et al*. Involvement and prognosis value of CD8(+) T cells in giant cell arteritis. *J Autoimmun* 2016;72:73–83.
- Graver JC, Abdulahad W, van der Geest KSM, *et al*. Association of the CXCL9-CXCR3 and CXCL13-CXCR5 axes with B-cell trafficking in giant cell arteritis and polymyalgia rheumatica. *J Autoimmun* 2021;123:102684.
- O'Neill L, Molloy ES. The role of toll like receptors in giant cell arteritis. *Rheumatology (Oxford)* 2016;55:1921–31.
- Deng J, Ma-Krupa W, Gewirtz AT, *et al*. Toll-like receptors 4 and 5 induce distinct types of vasculitis. *Circ Res* 2009;104:488–95.

- 37 Bonacini M, Rossi A, Ferrigno I, *et al.* The importance of defining which Janus kinases are activated in giant cell arteritis. *Clin Exp Rheumatol* 2023;41:784–6.
- 38 Zhang H, Watanabe R, Berry GJ, *et al.* Inhibition of JAK-STAT Signaling Suppresses Pathogenic Immune Responses in Medium and Large Vessel Vasculitis. *Circulation* 2018;137:1934–48.
- 39 Koster MJ, Crowson CS, Giblon RE, *et al.* Baricitinib for relapsing giant cell arteritis: a prospective open-label 52-week pilot study. *Ann Rheum Dis* 2022;81:861–7.
- 40 Terrier B, Geri G, Chaara W, *et al.* Interleukin-21 modulates Th1 and Th17 responses in giant cell arteritis. *Arthritis Rheum* 2012;64:2001–11.
- 41 Jiemy WF, van Sleen Y, van der Geest KS, *et al.* Distinct macrophage phenotypes skewed by local granulocyte macrophage colony-stimulating factor (GM-CSF) and macrophage colony-stimulating factor (M-CSF) are associated with tissue destruction and intimal hyperplasia in giant cell arteritis. *Clin Transl Immunology* 2020;9:e1164.
- 42 Cid MC, Unizony SH, Blockmans D, *et al.* Efficacy and safety of mavrimumab in giant cell arteritis: a phase 2, randomised, double-blind, placebo-controlled trial. *Ann Rheum Dis* 2022;81:653–61.
- 43 Ciccia F, Alessandro R, Rizzo A, *et al.* Expression of interleukin-32 in the inflamed arteries of patients with giant cell arteritis. *Arthritis Rheum* 2011;63:2097–104.
- 44 Field M, Cook A, Gallagher G. Immuno-localisation of tumour necrosis factor and its receptors in temporal arteritis. *Rheumatol Int* 1997;17:113–8.
- 45 Macaluso F, Marvisi C, Castrignanò P, *et al.* Comparing treatment options for large vessel vasculitis. *Expert Rev Clin Immunol* 2022;18:793–805.
- 46 Song GG, Lee YH. Efficacy and safety of biological agents in patients with giant cell arteritis: A meta-analysis of randomized trials. *Int J Clin Pharmacol Ther* 2020;58:504–10.
- 47 Deshayes S, Ly K-H, Rieu V, *et al.* Steroid-sparing effect of anakinra in giant-cell arteritis: a case series with clinical, biological and iconographic long-term assessments. *Rheumatology (Oxford)* 2021;61:400–6.
- 48 Ly K-H, Stirnemann J, Liozon E, *et al.* Interleukin-1 blockade in refractory giant cell arteritis. *Joint Bone Spine* 2014;81:76–8.
- 49 Zheng Y, Zhao J, Zhou M, *et al.* Role of signaling lymphocytic activation molecule family of receptors in the pathogenesis of rheumatoid arthritis: insights and application. *Front Pharmacol* 2023;14:1306584.
- 50 Karampetsou MP, Comte D, Kis-Toth K, *et al.* Expression patterns of signaling lymphocytic activation molecule family members in peripheral blood mononuclear cell subsets in patients with systemic lupus erythematosus. *PLoS One* 2017;12:e0186073.